Microbial Pathogenesis 173 (2022) 105843

Contents lists available at ScienceDirect

Microbial Pathogenesis

journal homepage: www.elsevier.com/locate/micpath

Pilus PilA of the naturally competent HACEK group pathogen *Aggregatibacter actinomycetemcomitans* stimulates human leukocytes and interacts with both DNA and proinflammatory cytokines

Nelli Vahvelainen [a], Esra Bozkurt [b], Terhi Maula [a], Anders Johansson [c], Marja T. Pöllänen [d], Riikka Ihalin [a,*]

[a] Department of Life Technologies, University of Turku, Turku, Finland
[b] Department of Biochemistry and Biophysics, Stockholm University, Stockholm, Sweden
[c] Division of Molecular Periodontology, Department of Odontology, Umeå University, Umeå, Sweden
[d] Institute of Dentistry, University of Turku, Turku, Finland

ARTICLE INFO

Keywords:
Aggregatibacter actinomycetemcomitans
Type IVa pilus
Cytokine
Host-pathogen interactions
Bacterial outer membrane proteins
Molecular models
Natural transformation systems

ABSTRACT

Each HACEK group pathogen, which can cause infective endocarditis, expresses type IVa pili. The type IVa major pilin PilA plays a role in bacterial colonization, virulence, twitching motility, and the uptake of extracellular DNA. The type IV prepilin homolog PilA of the periodontal pathogen *A. actinomycetemcomitans* (AaPilA) is linked to DNA uptake and natural competence.

Our aim was to investigate the virulence properties and immunogenic potential of AaPilA. Since *Neisseria meningitidis* PilE, which shares sequence similarity with AaPilA, participates in sequestering host cytokines, we examined the ability of AaPilA to interact with various cytokines. Moreover, we investigated the structural characteristics of AaPilA with molecular modeling.

AaPilA was conserved among *A. actinomycetemcomitans* strains. One of the 18 different natural variants, PilAD7S, is present in naturally competent strains. This variant interacted with DNA and bound interleukin (IL)-8 and tumor necrosis factor (TNF)-α. Specific anti-AaPilA antibodies were present in *A. actinomycetemcomitans*-positive periodontitis patient sera, and the production of reactive oxygen species from human neutrophils was less effectively induced by the Δ*pilA* mutant than by the wild-type strains. However, AaPilA did not stimulate human macrophages to produce proinflammatory cytokines, nor was it cytotoxic.

The results strengthen our earlier hypothesis that the DNA uptake machinery of *A. actinomycetemcomitans* is involved in the sequestration of inflammatory cytokines. Furthermore, AaPilA stimulates host immune cells, such as B cells and neutrophils, making it a potential virulence factor.

1. Introduction

Bacteria that are naturally competent for transformation can take up extracellular DNA and incorporate it to their own genome via homologous recombination. Efficient natural transformation requires molecular machinery that takes up DNA, as well as proteins that function in the recombination step to integrate the internalized DNA into the genome [1]. The uptake of extracellular DNA for transformation is mediated by type IV pili or structurally similar filamentous proteins [2]. The filament consists of subunits that polymerize and depolymerize at a rapid pace, extending from the periplasmic space to the extracellular space through a channel protein [3]. Although the pilus filaments are typically several micrometers long, the uptake of DNA does not necessarily require formation of a long pilus. Instead, the cells have been proposed to express a shorter pilus structure that is long enough to span the cell membrane and thus participate in the extracellular DNA uptake [4–6]. Expression of the pilin protein is necessary for natural transformation, even if the transformable cell would not express visible pilus filaments [7]. Type IV pili are needed for natural transformations that occur to acquire new genetic material, such as antibiotic resistance genes, in some human pathogens, such as *Vibrio cholerae* [8] and *Haemophilus influenzae* [9].

In addition to DNA uptake, the various functions of type IV pili in

* Corresponding author. Department of Life Technologies, BioCity 6th floor, Tykistökatu 6A, 20014, University of Turku, Finland.
E-mail address: riikka.ihalin@utu.fi (R. Ihalin).

https://doi.org/10.1016/j.micpath.2022.105843
Received 22 April 2022; Received in revised form 20 October 2022; Accepted 20 October 2022
Available online 27 October 2022

gram-negative bacteria include attachment to surfaces, microcolony formation, twitching motility, phage uptake, and electron transfer, which makes them important virulence factors for many human pathogens [10]. Major pilin proteins are required for virulence in *Francisella tularensis* [11], *Burkholderia mallei* [12] and *Burkholderia pseudomallei* [13]. Type IV pili promote adhesion to human cells and tissues, which thus promotes persistent infections. Adhesion and colonization are type IV pilus-mediated in *Kingella kingae* [14] and *Acinetobacter* species [15]. Moreover, meningococcal (*Neisseria meningitidis*)-type IV pili promote adhesion to human cells and tissues [16]. In addition to natural transformation, *H. influenzae* PilA plays a role in promoting adhesion, colonization, and stable biofilm formation [9,17]. Although *N. meningitidis* type IV major pilin PilE does not specifically interact with eDNA like the minor pilin ComP in a type IV pili heteromer [18], PilE has a role in cytokine uptake along with secretin PilQ [19].

Type IV pili are generally classified into type IVa and IVb pili, although a former subgroup of type IVb pili, the Flp family, has been reclassified as type IVc/tad pili [20–24]. The classification is based on the amino acid sequence of the major pilin subunit. In general, type IVa major pilins have shorter signal peptides (<10 amino acids (aa)) than type IVb and tad/IVc pilins (15–20 aa). The size of mature type IVa pilins is 150–175 aa on average, whereas type IVb pilins are larger (180–200 aa), and type IVc/tad pilins are smaller (approx. 50 aa) [20,23]. Type IV pilus and major pilin protein structures have been uncovered with crystallography, nuclear magnetic resonance, and cryoelectron microscopy [25–31]. The pilin proteins consist of an N-terminal α-helix and C-terminal globular domain. The conserved hydrophobic α-helix anchors the single pilins into the inner cell membrane during pilus assembly, and it is responsible for protein–protein interactions during the process. The globular domain is more diverse; however, an invariable structural element is a β-sheet consisting of 3–4 (type IVa) or 5–7 (type IVb) antiparallel strands. The C-terminus also harbors a hypervariable D-region defined by two conserved cysteines that form a disulfide bond. The D-region of type IVb pilin proteins is typically longer and has more defined structural elements than type IVa pilins. The D-region of pilins can have structural and/or functional roles that vary between proteins due to hypervariability [20]. Only type IVa pili have been associated with DNA uptake during natural transformation [2]. Additionally, type IVa pili are associated with motility, whereas type IVb and IVc/tad pili play a role in adhesion, microcolony formation, secretion and DNA exchange by conjugation and phage DNA acquisition [32].

Periodontitis is an oral infection caused by a dysbiotic, mainly gram-negative biofilm [33]. Although the development of periodontitis requires the overgrowth of subgingival biofilms, some gram-negative bacterial species, such as *Porphyromonas gingivalis*, *Tannerella forsythia*, *Treponema denticola* and *Aggregatibacter actinomycetemcomitans*, most likely possess virulence factors that can shift the balance toward dysbiosis and the progression of inflammation in tooth-supporting tissues [33]. Of these species, *A. actinomycetemcomitans* belongs to the HACEK group (*Haemophilus*, *Aggregatibacter*, *Cardiobacterium*, *Eikenella*, *Kingella*) of gram-negative bacteria, which can cause infective endocarditis. All these species express type IVa pili, which are involved in the virulence of *H. influenzae* [17], twitching motility of *E. corrodens* [34] and colonization of *Kingella* [14].

The naturally competent strains of *A. actinomycetemcomitans* require a type IV prepilin homolog PilA for natural transformation: *pilA* is expressed in competence-inducing conditions, and deletion of the gene results in a nontransformable strain [35]. Although PilA is homologous to type IV major pilin proteins it does not form visible pilus filaments [35]. Therefore, PilA is not involved in fimbria expression of *A. actinomycetemcomitans*. Instead, fimbria expression is dependent on another type IV pili, the Flp pili, that is different from PilA [24]. Flp belongs to the IVc/tad group of short, tight adherence pili [22,24], whereas, as we show in this study, PilA resembles type IVa pilins.

To the best of our knowledge, functional studies with recombinant PilA have not been performed, and there is no information on whether *A. actinomycetemcomitans* PilA has some virulence-related characteristics. Our earlier studies indicate that *A. actinomycetemcomitans* can sequester host cytokines, such as interleukin (IL)-1β and IL-8 [36–38]. *A. actinomycetemcomitans* possesses an *N. meningitidis* PilQ homolog, the outer membrane secretin protein HofQ, which interacts with double-stranded DNA and most likely forms the channel through which a pilus extends [39]. Moreover, we have shown that HofQ binds human cytokines [40]. Since the PilA homolog PilE of *N. meningitidis*, together with the secretin PilQ, participates in the internalization of host cytokines [19], we hypothesize that the *A. actinomycetemcomitans* PilA plays a role in the uptake of cytokines.

In this study, we used recombinant proteins and whole *A. actinomycetemcomitans* cells to study the possible diverse functions of *A. actinomycetemcomitans* PilA. PilA has several natural variants, but in this study, we focused on the one variant that is present in the naturally competent strains, as we have previously proposed a link between natural competence and cytokine uptake [40]. The amino acid sequences were examined to observe the similarities between PilA and known type IV pilins, and thus determine which class of type IV pili PilA belongs to. Because PilA has been shown to be important in natural transformation, we investigated its interaction with DNA. In addition to eDNA, *A. actinomycetemcomitans* has been shown to internalize cytokines [37], and because the PilA homolog, type IV pilus PilE of *N. meningitidis* has been shown to take part in cytokine internalization [19], we used recombinant proteins to study interactions between human cytokines and PilA. Various type IV pili, which are homologous to PilA, stimulate human leukocytes. Therefore, we stimulated human neutrophils and macrophages with whole *A. actinomycetemcomitans* cells and recombinant PilA proteins, respectively. Additionally, we measured whether PilA elicits antibody production in the sera of *A. actinomycetemcomitans*-positive periodontitis patients.

This study shows that *A. actinomycetemcomitans* PilA resembles type IVa major pilin proteins. PilA interacted with DNA, which supports its role in natural transformation, and bound human cytokines, suggesting that it mediates the uptake of cytokines. Additionally, PilA showed immunogenic and antigenic properties, as it stimulated human neutrophils to produce reactive oxygen species (ROS) and elicited specific antibody production.

2. Materials and methods

2.1. Bacterial strains

Recombinant proteins were expressed in the *Escherichia coli* BL21 CodonPlus (DE3)RIL strain (Stratagene). The *A. actinomycetemcomitans* D7S wild-type strain [41], deletion mutant strain D7S Δ*pilA::spe*^{r} [35] and D11S wild-type strain [42] were a kind gift from Professor Casey Chen (USC, Los Angeles, USA).

2.2. Expression and purification of recombinant proteins

The genes encoding mature PilAD7S (amino acids 1–134), PilAD7S (Δ1–23) (amino acids 24–134) and PilAD7S(Δ1–27) (amino acids 28–134) were ordered as codons optimized for *E. coli* K12 (Table 1) from Eurofins Genomics (Ebersberg, Germany). The genes contained restriction sites for NdeI and XhoI, which were used to clone the genes into the expression vector pET-15b (Novagen), which contains an N-terminal His-tag with a thrombin digestion site. The expression constructs were verified by sequencing (Eurofins Genomics) and transformed into *E. coli* BL21 CodonPlus (DE3)RIL.

Proteins were expressed in Terrific Broth (TB; 12 g/l tryptone, 24 g/l yeast extract, 0.4% glycerol, 17 mM KH_2PO_4, 72 mM K_2HPO_4) supplemented with 100 μg/ml ampicillin and 30 μg/ml chloramphenicol. Cells were grown at 23 °C for 6–8 h to approx. $OD_{600nm} = 1.5–2.0$, and protein production was induced with 1 mM isopropyl β-D-1-thiogalactopyranoside (IPTG). After induction, the cells were grown at 16 °C overnight and

Table 1
The *pilA* gene sequences were optimized for recombinant protein expression in *E. coli*. Restriction enzyme recognition sites used in cloning are underlined.

pilAD7S	CAT ATG TTT ACC CTG ATC GAA CTC ATG ATT GTG ATT GCG ATT GTG GCC ATT CTG GCC ACT GTG GCA GTT CCG AGC TAT CAG AAC TAC ACC AAG AAA GCA GCA GTC TCG GAA TTG CTG CAA GCG AGT GCT CCG TTA CGC TCT GAA GTT GAG CTG TGC ATC TAT AAC ACC GGT AAA GCG GAG AAC TGT TCC GGA GGT CAG AAT GGC ATT CAA GCC GAT GTA GCC GAT GCG TCC AAA CAG AAG TAC GTC AAA AGT ACG GCT GTG AAA GGA GGC GTC ATT ACC GTA ACC GGG AAA GGC TCT CTG GAC AAA ATC TCG TAT ACG CTT ACG GCG TCA GGT ACA GCC GCT ACT GGC GTT AGC TGG AAT GCG GCA TGT GGG AAC AAT GCG GGC ATC TTT CCA GCC GGT TTC TGC AGC TAA CTC GAG
pilAD7S (Δ1–23)	CAT ATG TAT CAG AAC TAC ACG AAG AAA GCC GCT GTA TCC GAA CTC TTG CAA GCG TCA GCT CCG TTA CGC TCC GAA GTG GAA CTG TGC ATC TAT AAC ACG GGT AAA GCG GAG AAC TGT AGT GGA GGA CAG AAT GGC ATT CAA GCC GAT GTT GCG GAT GCC TCG AAA CAG AAG TAC GTC AAA AGC ACC GCG GTG AAA GGT GGG GTG ATT ACC GTT ACC GGC AAA GGT TCG CTG GAC AAA ATC AGC TAT ACC CTG ACT GCA TCT GGT ACT GCA GCT ACA GGC GTC AGT TGG AAT GCG GCC TGT GGG AAC AAT GCG GGC ATT TTC CCA GCA GGC TTT TGC AGC TAA CTC GAG
pilAD7S (Δ1–27)	CAT ATG ACC AAG AAA GCG GCT GTT AGC GAA CTC CTG CAA GCG TCA GCA CCG TTA CGC AGT GAA GTG GAA CTG TGC ATC TAT AAC ACG GGA AAA GCC GAG AAC TGT AGT GGT GGT CAG AAT GGC ATT CAG GCC GAT GTA GCG GAT GCG TCC AAA CAG AAG TAC GTC AAA TCC ACC GCA GTG AAA GGA GGT GTC ATT ACC GTG ACT GGG AAA GGC AGC TTG GAC AAA ATC TCG TAT ACG CTG ACA GCC TCT GGC ACT GCA GCC ACC GGT GTT TCG TGG AAT GCT GCG TGT GGC AAC AAT GCG GGG ATT TTC CCA GCT GGC TTT TGC AGC TAA CTC GAG

harvested by centrifugation (6,400×*g*, 10 min, 4 °C). Pelleted cells were stored at −20 °C.

To purify the recombinant proteins, 25 g cells were thawed and suspended in 100 ml of binding buffer (20 mM Na-phosphate buffer, 300 mM NaCl, 20 mM imidazole, pH 8.0) supplemented with 1 μg/ml DNase I (Roche Diagnostics GmbH, Mannheim, Germany), 0.2 mM protease inhibitor phenylmethylsulfonyl fluoride (PMSF; Sigma) and 10 mM $MgCl_2$. The cell suspension was sonicated 4 × 30 s with a 12 μm amplitude (100 Watt MSE Ultrasonic disintegrator), and the cell debris was removed by centrifugation (48,000×*g*, 30 min, 4 °C). The supernatant containing soluble proteins was loaded into a nickel-loaded 5 ml HisTrap™ HP column (#17-5248-01, GE Healthcare) equilibrated with binding buffer. The column was washed with binding buffer to remove unbound proteins. His-tagged proteins were eluted with elution buffer (20 mM Na-phosphate buffer, 300 mM NaCl, 300 mM imidazole, pH 7.5). The eluate was further purified by size-exclusion chromatography in a gel filtration column (HiLoad® 26/600 Superdex® 200 pg, #28-9893-36, GE Healthcare) equilibrated with phosphate buffered saline (PBS: 140 mM NaCl, 2.7 mM KCl, 10 mM Na_2HPO_4, 1.8 mM KH_2PO_4, pH 7.4). Fractions containing the desired protein were pooled and concentrated with a centrifugal filter device with a 10 kDa cutoff (Amicon® Ultra15 Centrifugal Filter Unit, Millipore). The protein concentration was measured using a method described by Lowry and coworkers [43], and the protein was stored at −80 °C.

To cleave the N6-His-tag, 200 units of thrombin (MP Biomedicals, Santa Ana, CA, USA) were added to the HisTrap column prior to elution. The column was incubated overnight at RT, and the cleaved proteins were eluted with binding buffer. Purification was continued with size-exclusion chromatography as described above.

The production and purification of recombinant human mature IL-8 has been described by Ahlstrand and coworkers [38]. Purification of His-tagged IL-8 was performed similarly to His-tagged PilA protein purification (described above). The production and purification of recombinant emHofQ has been described by Ahlstrand and coworkers [40].

The size and purity of the produced recombinant proteins were determined by SDS-PAGE: 2 μg of protein was mixed with SDS sample buffer (final concentration 62.5 mM Tris-HCl pH 6.9, 2% SDS, 18% glycerol, 0.01% bromophenol blue, 0.1% β-mercaptoethanol), incubated at 100 °C for 5 min and run on a 10% Criterion™ TGX™ Precast Midi Protein Gel (#5671034, BioRad). The gel was stained with Bio-Safe Coomassie G-250 Stain (#1610786, BioRad) according to the manufacturer's instructions.

2.3. Detecting aggregation with western blotting

Recombinant His-tagged PilAD7S, PilAD7S(Δ1–23) or PilAD7S (Δ1–27) were crosslinked with formaldehyde. Recombinant proteins (100–200 ng/μl) in PBS were incubated with 1% formaldehyde at RT for 30 min, and the reaction was stopped by adding SDS sample buffer and incubating at 100 °C for 5 min. Cross-linked protein aggregates were separated by size with SDS-PAGE (12% Criterion™ TGX™ Precast Midi Protein Gel, #5671044, BioRad). Proteins were transferred to a nitrocellulose membrane with a semidry transfer (90 mA for 2 h), and the membrane was blocked with 2.5% BSA in Tris buffered saline (TBS: 25 mM Tris, 150 mM NaCl, pH 7.6) with 0.05% Tween-20 (TBS-T) overnight at 4 °C. The membrane was washed three times for 5 min with TBS-T and incubated with 1 μg/ml His-Probe HRP (#15165, Thermo Scientific) (diluted in TBS-T with 2.5% BSA) for 2 h at RT in the dark. The membrane was washed four times for 10 min with TBS-T and incubated for 1 min with chemiluminescence enhancing solution (Pierce™ ECL Western blotting substrate; #32106, Thermo Scientific). The light reaction was detected by incubating the membrane with a light-sensitive film and developing the film with Kodak reagents.

2.4. DNA-binding assay (electrophoretic mobility shift assay; EMSA)

The interaction between recombinant PilA and linearized USS plasmid (dsDNA) was examined with EMSA as described by Tarry and coworkers [39]. Recombinant PilAD7S(Δ1–27) (100 μg, without His-tag) and linearized USS DNA (300 ng) were incubated together at RT for 30 min. Recombinant emHofQ (100 μg) and BSA (100 μg) were used as positive and negative controls, respectively. Samples were run on a 1.2% agarose gel at 70 V for 2.5 h. The DNA bands were visualized with Midori Green Advance stain (#MG04, Nippon Genetics Europe) under UV light.

2.5. Cytokine binding assay (ELISA)

Wells of a 96-well plate (Nunc Maxisorp, Thermo Fisher Scientific) were coated with 50 μl of cytokine dilutions (IL-8 (in house), TNF-α (ReliaTech, Wolfenbüttel, Germany); 120 μM) in PBS-N (PBS with 0.05% sodium azide) at 4 °C for 3 days. BSA (30 μM) was used as a negative control. The wells were washed three times with distilled water, and empty binding sites were blocked with 0.25% BSA in PBS-T (PBS with 0.05% Tween-20) at 37 °C for 3 h. The wells were washed three times with distilled water, and N6-His-tagged PilAD7S(Δ1–27) was added at different concentrations. His-tagged emHofQ was used as a positive control, and PBS was used as a negative control. The plate was incubated at 4 °C overnight. The wells were washed with PBS-T using a DELFIA® Platewash (PerkinElmer). For detection, 50 μl of 2 μg/ml His-Probe HRP (#15165, Thermo Scientific) in PBS-T was added, and the plate was incubated at RT in the dark for 30 min. The wells were washed with PBS-T as described above, and 100 μl of 1 mM 2,2′-azino-bis(3-ethylbenzothiazoline-6-sulfonic acid) diammonium salt (#A9941, Sigma-Aldrich) in 10 mM sodium citrate buffer (pH 4.2) supplemented with 0.03% H_2O_2 was added to the wells. The color change was detected by measuring the absorbance at 405 nm after 60 min with a Multiskan Go plate reader (Thermo Scientific). The test was conducted five times with technical triplicates. The binding constant was determined with the Hill function.

2.6. Time-resolved fluorometric immunoassay (TRFIA)

Wells of a 96-well plate (Nunc Maxisorp, Thermo Fisher Scientific)

were coated with 86 pmol of recombinant PilAD7S(Δ1–27). Recombinant emHofQ was used as a positive control. The plate was incubated at 4 °C overnight, and the wells were washed once with PBS using a DELFIA® Platewash. Empty binding sites were blocked with 200 μl Alternative Block (#6299, ImmunoChemistry Technologies, Bloomington, MN, USA) overnight at RT. Alternative Block was also added to empty wells to obtain the fluorescence background. The wells were washed three times with PBS-T using Platewash. His-tagged recombinant human IL-8 (0–9.3 μM) in DELFIA Assay Buffer (#4002-0010, PerkinElmer) was added to the wells and incubated overnight at 4 °C. Additionally, recombinant IL-8 (6.1–9.3 μM) was added to noncoated, nonblocked wells as a positive control. The wells were washed with PBS-T as mentioned above, and 25 ng DELFIA® Eu-N1 Anti-6xHis antibody (#AD0108, PerkinElmer) diluted in 50 μl DELFIA® Assay Buffer was added to the wells and incubated for 1 h at RT. The wells were washed as mentioned above. Then, 100 μl DELFIA® Enhancement Solution (#1244-105, PerkinElmer) was added to the wells. After 5 min of incubation, time-resolved fluorescence was measured with a VICTOR^3 Multilabel Plate Counter (PerkinElmer). The test was conducted five times in triplicate. The results were standardized by comparing the fluorescence values to a control value (fluorescence of 6.1 μM IL-8 in DELFIA® Assay Buffer in noncoated wells) in each individual test after subtracting the fluorescence background. The binding constant was determined with the Hill function.

2.7. Human serum and leukocyte collection

For screening antibodies in the sera, human venous blood was collected from *A. actinomycetemcomitans*-positive adult periodontitis patients (n = 21) and healthy control subjects (n = 14) as previously described [40]. Human venous blood for isolating leukocytes and plasma for the ROS production assay were collected from healthy volunteers (n = 7) with the same exclusion criteria as above. All patients and healthy persons provided written informed consent prior to sample collection. Collection was conducted by a laboratory nurse at the Community Dental Healthcare Center of Turku (Institute of Dentistry, University of Turku) or by a physician at the Unit for Specialized Oral Care in the Helsinki Metropolitan Area and Kirkkonummi (Helsinki, Finland).

2.8. Screening of A. actinomycetemcomitans PilA-specific antibodies

A. actinomycetemcomitans PilA-specific antibodies in human sera were screened using ELISA as previously described [40]. Briefly, the wells were coated with recombinant PilAD7S(Δ1–27) (500 ng) or BSA (500 ng), and empty binding sites were blocked with BSA-containing buffer. Patient and control sera (1/20 dilutions) were added and incubated overnight at RT, which was followed by additional blocking for 10 min at RT. The bound human IgG antibodies were detected with anti-human IgG (Fc specific) peroxidase-coupled antibody (#A1070, Sigma Aldrich). Peroxidase was detected as described above in the "Cytokine binding assay (ELISA)".

Initial testing was conducted with two sera per plate in three different dilutions: 1/20, 1/50 and 1/100. The 1/20 dilution was chosen for the final assays, which were performed in triplicate. The results were obtained from 21 *A. actinomycetemcomitans*-positive patient sera and 14 healthy control sera. Nonspecific binding to BSA was subtracted from the values obtained for PilA binding.

2.9. ROS production induced by A. actinomycetemcomitans

Reactive oxygen species (ROS) production of human leukocytes induced by the *A. actinomycetemcomitans* D7S wild-type, D11S wild-type and D7S Δ*pilA*::*spe*^{r} mutant strains was measured with luminol-enhanced chemiluminescence [40,44]. Briefly, 100 μl of *A. actinomycetemcomitans* suspension (1.25 × 10^7 CFU) in gHBSS (1 mg/ml gelatin in HBSS: 1 mM $CaCl_2$, 5 mM KCl, 0.4 mM KH_2PO_4, 0.5 mM $MgCl_2$•6 H_2O, 0.4 mM $MgSO_4$•7 H_2O, 140 mM NaCl, 4 mM $NaHCO_3$, 0.3 mM Na_2HPO_4, 6 mM glucose) was added to the wells of a white 96-well plate (#391-3103, Greiner Bio-One) and incubated at RT for 40 min. Luminol, human plasma, and freshly isolated human leukocytes were added to the wells, and luminescence was measured every 2 min with a VICTOR^3 multilabel plate counter (Perkin Elmer) until the peak values were obtained. Plasma was obtained from the same healthy volunteer for every test, whereas leukocytes were isolated from a different healthy volunteer (n = 6–7) every time. The peak values of the luminescence signals were compared.

2.10. Macrophage stimulation assay

Macrophage stimulation assays were performed as previously described [45] using THP-1 human acute monocytic leukemia cells (ATCC® TIB-202™) [46]. Briefly, 2 × 10^5 THP-1 monocytes (passages 12–24) were differentiated into a macrophage-like phenotype with 50 nM phorbol 12-myristate 13-acetate (PMA; #5.00582, Sigma-Aldrich) for 24 h. The cells were washed with PBS (#D8537, Sigma-Aldrich) and incubated in fresh medium for an additional 24 h. Recombinant PilAD7S(Δ1–27) (without His-tag) and LPS from *A. actinomycetemcomitans* [47] were diluted 0.1 ng/ml in RPMI and incubated at RT for 1 h. Macrophages were washed with PBS and incubated in 200 μl of stimulation agent for 6 h or 24 h. The medium was collected and stored at 20 °C. Cytokine concentrations in the medium samples were measured with Single-Analyte ELISArray™ Kits (Qiagen). The test was conducted five times in triplicate.

Cell viability was measured with the neutral red uptake assay [48] immediately after medium collection. Briefly, the cells were washed with PBS and incubated with 100 μl of 40 μg/ml neutral red dye for 90 min. The cells were washed with PBS and destained with lysis solution (EtOH:MQ:acetic acid at 50:49:1 (v/v)) for 30 min at RT. The absorbance at 540 nm was used to measure the amount of dye released.

2.11. Bioinformatics

Sequence similarity searches were performed with NCBI BLAST [49]. Multiple sequence alignments were performed using Clustal Omega [50]. Sequence alignments were edited and/or visualized with the BioEdit sequence alignment editor (Informer Technologies, Inc.).

2.12. Statistics

The statistical analyses were performed with IBM SPSS Statistics (versions 26 and 27). Statistical differences between more than two groups were analyzed with the nonparametric Kruskal–Wallis test, followed by paired Mann–Whitney U tests with Bonferroni correction when there was a significant difference. Statistical differences between two groups were analyzed with the Mann–Whitney *U* test. Differences were regarded as statistically significant at $p \leq 0.05$.

2.13. Computational details

The pilus subunits that exhibit a C-terminally truncated β-sheet fold of the immunoglobulin domains common in many other proteins [51] were modeled using AlphaFold [52], which utilizes novel neural network architectures and training procedures to predict protein structures with high accuracy. The protonation states of charged residues were assigned at pH 7.4, and hydrogen atoms were added using the H++ webserver [53]. Molecular dynamics (MD) simulations were carried out using the Amber18 molecular dynamics package [54], and the ff14SB [55] force field was employed for the parametrization of protein residues. Monomeric proteins were solvated with a TIP3P [56] water model, and sodium and/or chloride atoms were added to maintain the neutrality of the systems. The resulting systems were minimized to

remove any poor contacts between the solute and solvent. Next, the systems were heated from 50 K to 300 K with a timestep of 2 fs using weak restraints on the backbone and sidechain atoms. Restraints were gradually released within 5 ns, followed by molecular dynamics simulations (250 ns) at a constant temperature of 300 K with a timestep of 2 fs. The temperature was maintained by a Langevin [57] thermostat. A cutoff of 12 Å was used for nonbonded interactions, and the long-range interactions were treated by the particle mesh Ewald (PME) method [58,59]. The SHAKE [60] algorithm was applied to constrain the bonds involving hydrogen atoms. The protein structures were clustered over the last 50 ns of the corresponding MD simulations using the CPPTRAJ [61,62] utility in the AMBER suite. The representative frame of the most populated cluster was selected to represent the final monomeric protein structures. We used the K-means algorithm to cluster based on the RMSD (C, N, O, CA, CB) of protein residues.

Although *A. actinomycetemcomitans* PilA has not been shown to form visible pilus filaments [35], similar pilin proteins do form multimers [29,31]. Additionally, as PilA is needed for natural transformation, it likely forms multimers that are long enough to span the cell membrane and bind the extracellular DNA [4–6]. Therefore, we modeled a homo-oligomeric structure of PilAD7S. The computational details and the resulting predicted structure of a homo-oligomeric *A. actinomycetemcomitans* PilA are described in Supplemental information.

2.14. Ethics statement

Permission to collect and use the blood samples of *A. actinomycetemcomitans*-positive periodontitis patients and healthy control subjects for antibody screening (approval #61/180/2009) and to collect and use the blood samples from healthy volunteers for ROS production assays (approval #151/1801/2014) was obtained from the Ethics Committee of the Hospital District of Southwest Finland. Written informed consent was obtained from every periodontitis patient and healthy individual to collect venous blood samples.

3. Results

3.1. Highly conserved A. actinomycetemcomitans PilA (AaPilA) shares sequence similarity with type IVa pilins

The amino acid sequences of *A. actinomycetemcomitans* strain D7S

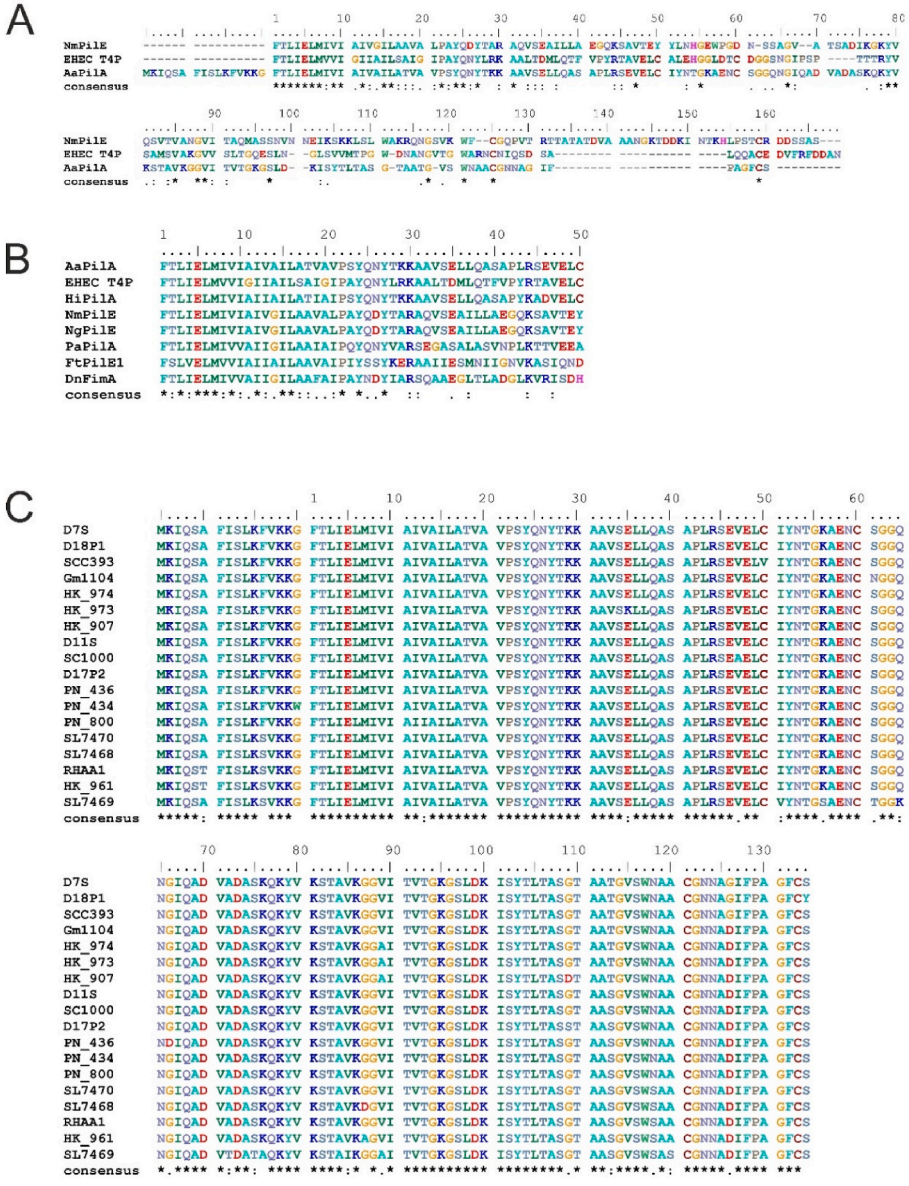

Fig. 1. A) Conserved *A. actinomycetemcomitans* PilA (AaPilA) shared sequence similarity with two type IVa pilin proteins, *N. meningitidis* PilE (NmPilE) and EHEC T4P, mostly in the N-terminus. B) The N-terminal sequence of AaPilA was highly similar also to other known type IV pilins from gram-negative species (Hi: *H. influenzae*, Ng: *Neisseria gonorrhoeae*, Pa: *Pseudomonas aeruginosa*, Ft: *F. tularensis*, Dn: *Dichelobacter nodosus*). C) Altogether, 18 different AaPilA variants could be found among the 95 fully or partially sequenced *A. actinomycetemcomitans* strains. These variants were highly conserved, showing ≥90% identity. The sequence follows mature protein numbering starting with phenylalanine (F) at position 1. The first 16 amino acids form the signal peptide.

PilA, *N. meningitidis* type IVa pilin PilE (PDB ID 5kua [29]) and enterohemorrhagic *E. coli* type IVa pilin (PDB ID 6gv9 [31]) were aligned with Clustal Omega (Fig. 1A). Alignment in the C-terminal region was manually adjusted to align the two conserved cysteines that define the hypervariable D-region in type IV pilins [20]. The alignment revealed high similarity in the N-terminus, whereas the C-terminal part was more variable. The N-terminal mature amino acid sequence of AaPilA was further aligned with sequences of other type IVa pilins from gram-negative species to reveal high sequence similarity (Fig. 1B).

The amino acid sequence of AaPilA strongly resembles that of type IVa pilin proteins, which have a highly conserved hydrophobic N-terminus [3]. Although AaPilA has a relatively long signal peptide (16 aa), the mature pilin size is 134 aa. Additionally, the first residue of the mature pilin is phenylalanine, which is conserved with type IVa major pilins [20]. Moreover, in AaPilA, there are only 11 aa between the two C-terminal cysteines, which defines the hypervariable D-region. This also suggests that AaPilA is a type IVa pilin because type IVb pilins have long, structurally defined D-regions [20].

Among the 95 completely or partially sequenced *A. actinomycetemcomitans* strains (retrieved from GenBank on March 10th, 2021), 18 different PilA variants were found (Fig. 1C). PilA was highly conserved, as the variants were at least 90% identical to each other. Additionally, PilA variants could be divided into four clusters based on amino acid similarity. Inside these clusters, the protein variants were at least 98.7% identical to each other and had a max. 2 aa difference. Two variants were clearly more abundant than the remaining 16. These two variants, PilAD7S and PilAD11S (named after one of the strains they are expressed in), were present in 28 (29%) and 36 (38%) strains, respectively. Majority of serotype b and c strains express PilAD11S, whereas PilAD7S is expressed mainly in serotype a and d strains. Serotype a has been linked with natural competence while serotype b and c strains are not competent for transformation [63]. Moreover, PilAD7S is present in the naturally competent serotype a strains D7S, 624, and D17P-3 [1], and as we hypothesize that DNA uptake during natural transformation and cytokine uptake are linked [40], we focused on the D7S variant in this study.

3.2. Predicted structures of monomeric AaPilA resemble type IVa pili

To understand the monomeric structures of PilAD7S(Δ1–27) and PilAD7S at the molecular level, we performed computational modeling studies. The predicted structures of PilAD7S(Δ1–27) and PilAD7S share essentially the same secondary structural elements and are simply composed of one N-terminal α-helix, four antiparallel β-strands, a hypervariable segment and a flexible C-terminus (Fig. 2A and B). Slight disparities are present in the hypervariable and loop regions. The interfaces between the helices and one of the β-strands consist mainly of hydrophobic valine, leucine, and isoleucine residues. Overall, both predicted monomeric structures are highly similar and are superimposed with a root mean square deviation of 0.78 Å for the CA main chain atoms.

3.3. Hydrophobic N-terminal α-helix causes aggregation in recombinant proteins

The purity of the produced recombinant PilA proteins was confirmed with SDS-PAGE (Fig. 3A). The recombinant protein sizes (N6-His-tagged/without His-tag) were as follows: PilAD7S 15.6 kDa/14.1 kDa, PilAD7S(Δ1–23) 13.2 kDa and PilAD7S(Δ1–27) 12.7/11.2 kDa.

PilA has a hydrophobic N-terminal α-helix that decreases the solubility of recombinantly produced proteins and likely causes them to aggregate (Fig. 3B). To avoid aggregation, we produced two N-terminally truncated recombinant variants: PilAD7S(Δ1–23) and PilAD7S (Δ1–27). These proteins lack the first 23 or 27 amino acids of the mature sequence of PilAD7S, respectively. Cross-linking tests revealed that the N-terminally truncated variants formed significantly smaller protein aggregates (only up to 35 kDa) than the full-length PilA (over 250 kDa) (Fig. 3B). The formaldehyde link is only 12 Da in size and thus did not significantly increase the size of the protein complexes. The N-terminally truncated variant PilAD7S(Δ1–27) was used in some experiments to avoid problems caused by aggregation.

3.4. Recombinant PilA binds linear A. actinomycetemcomitans DNA

Some *A. actinomycetemcomitans* strains are naturally competent, *i.e.*,

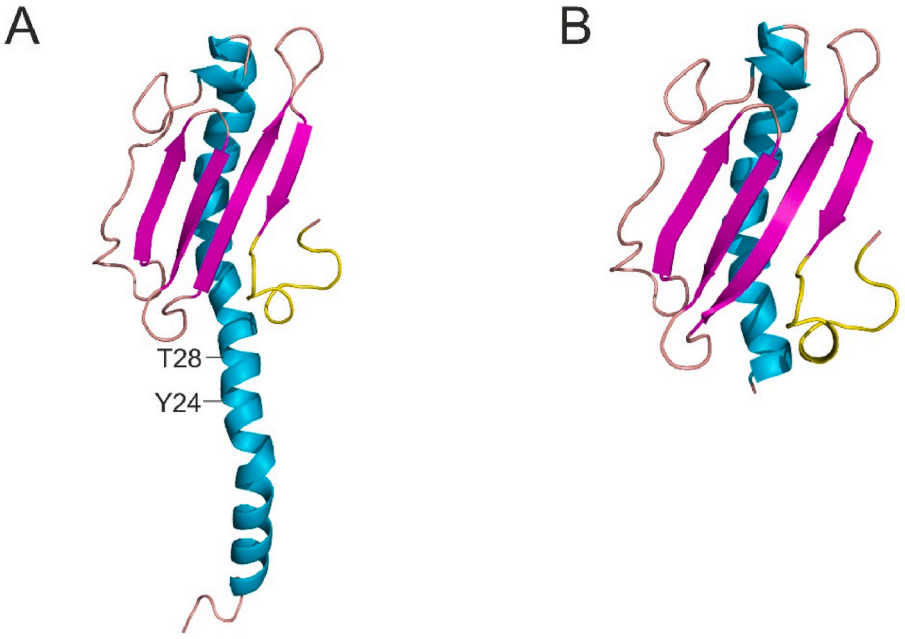

Fig. 2. Computationally predicted 3D structures of monomeric PilAD7S and N-terminally truncated PilAD7S(Δ1–27). A) Monomeric PilAD7S has an N-terminal α-helix, four antiparallel β-sheets and a hypervariable D-region at the C-terminus. B) PilAD7S(Δ1–27) has essentially the same structures, except for a truncated α-helix.

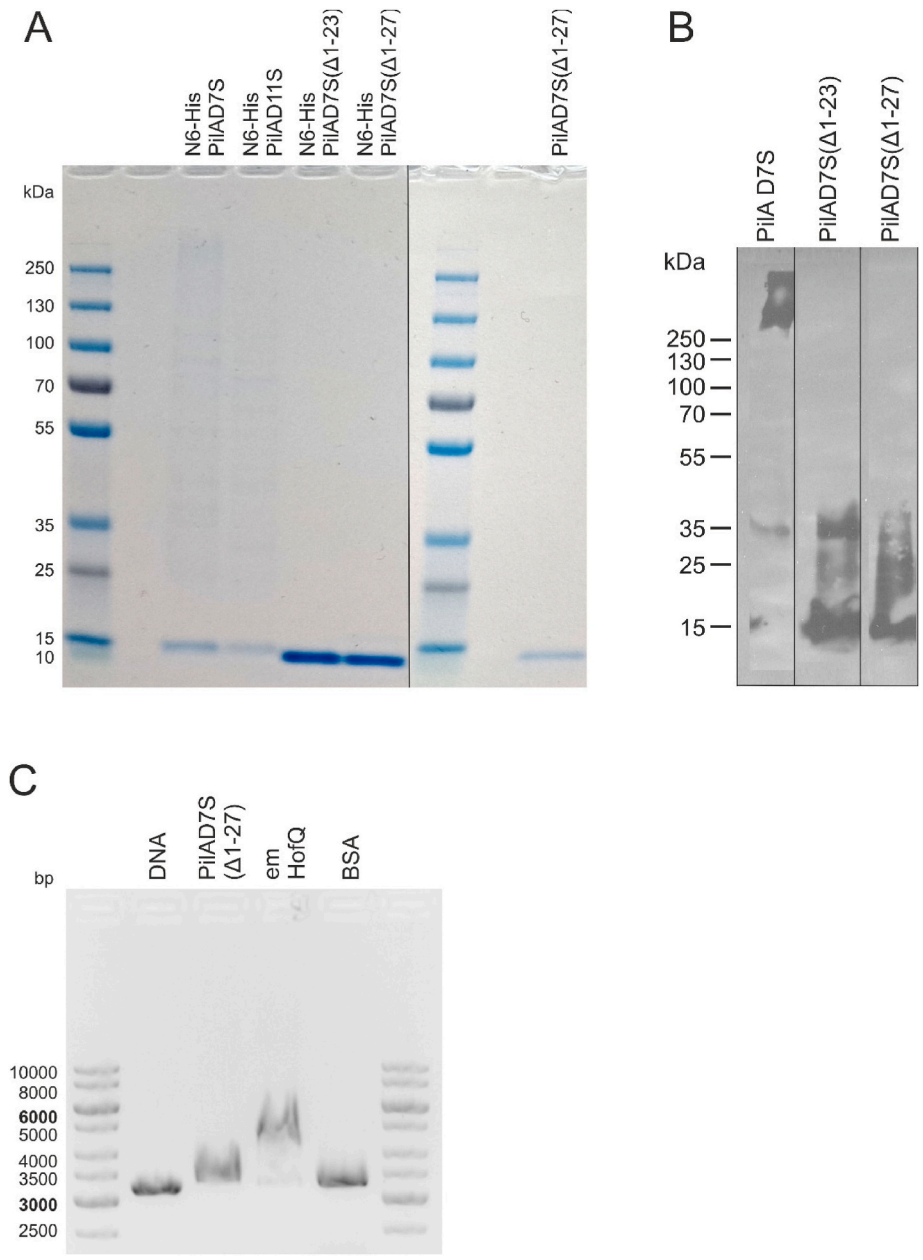

Fig. 3. A) The purity and size of the produced PilA proteins were confirmed with SDS-PAGE. B) Full-length PilAD7S formed large aggregates, which was avoided with truncated variants PilAD7S(Δ1–23) and PilAD7S(Δ1–27). C) The N-terminally truncated PilAD7S(Δ1–27) interacted with linear DNA, which contained an *A. actinomycetemcomitans*-specific uptake signal sequence (USS). Recombinant emHofQ and BSA were used as positive and negative controls, respectively.

they can take up extracellular DNA and incorporate it into their genome via homologous recombination. The first gene cluster that was associated with the natural competence of *A. actinomycetemcomitans* was *pilABCD* [35]. Additionally, *A. actinomycetemcomitans* preferentially internalizes DNA that contains a specific uptake signal sequence (USS) that is abundant in the genomic DNA of many *Haemophilus* species [64]. Therefore, we tested whether *A. actinomycetemcomitans* PilA binds linearized USS containing dsDNA. Recombinant, N-terminally truncated PilAD7S(Δ1–27) interacted with DNA (Fig. 3C). Binding was observed as a mobility shift in an agarose gel.

3.5. Recombinant PilA binds human IL-8 and TNF-α

N. meningitidis PilE, a protein homolog of PilA, is involved in the uptake of human proinflammatory cytokines [19]. Since *A. actinomycetemcomitans* is known to internalize cytokines [37], we wanted to study whether PilA is involved in this process. Due to the formation of protein aggregates, comprehensive investigation of binding was not feasible with full-length recombinant PilA. To determine the dissociation constants, we used the N-terminally truncated PilAD7S (Δ1–27). Binding to TNF-α was studied with ELISA using immobilized TNF-α and His-tagged PilAD7S(Δ1–27). The dissociation constant was determined to be 7.16 ± 0.40 μM (Fig. 4A). IL-8 binding was studied with TRFIA using immobilized PilAD7S(Δ1–27) and His-tagged IL-8. The dissociation constant was determined to be 0.67 ± 0.18 μM (Fig. 4B).

3.6. The sera of A. actinomycetemcomitans-positive periodontitis patients contained PilA-specific antibodies

We have shown that *A. actinomycetemcomitans*-positive periodontitis patients have significantly higher amounts of *A. actinomycetemcomitans*-

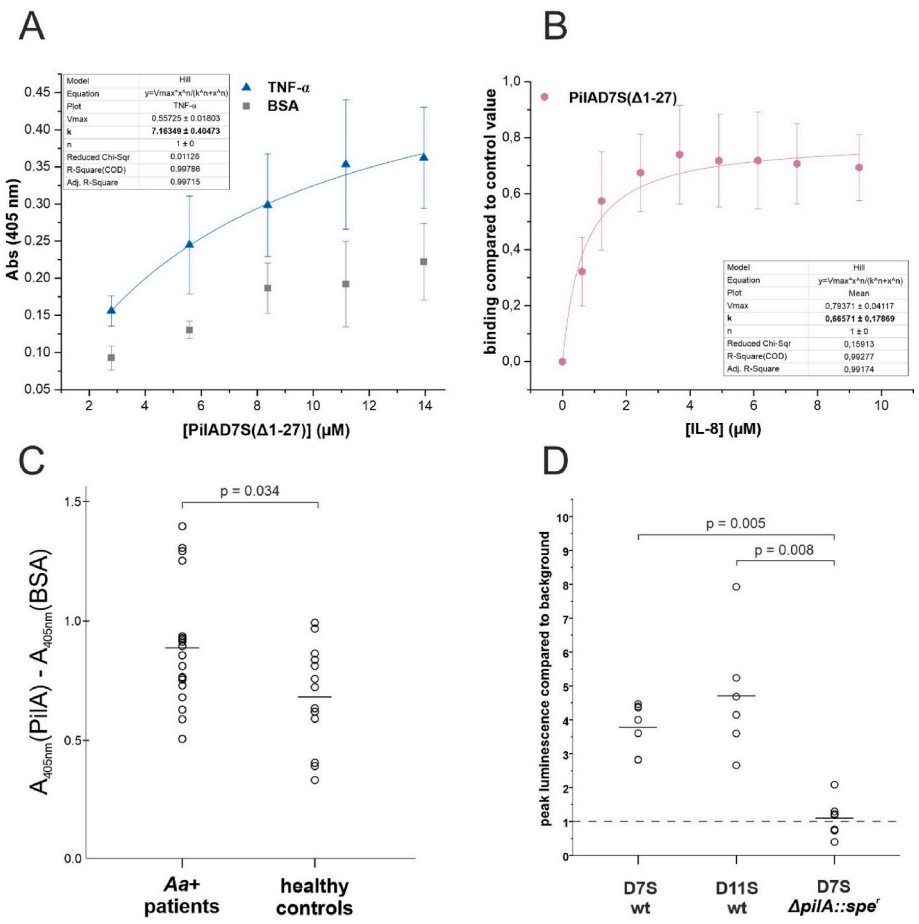

Fig. 4. *A. actinomycetemcomitans* PilA interacted with cytokines and exhibited immunogenic properties. The N-terminally truncated variant PilAD7S(Δ1–27) interacted with A) TNF-α and B) IL-8 with K_d values of 7.16 ± 0.40 μM and 0.67 ± 0.18 μM, respectively. C) *A. actinomycetemcomitans*-positive periodontitis patient sera (N = 21) contained higher levels of AaPilA-specific antibodies than healthy control sera (N = 14) (p = 0.034; Mann–Whitney *U* test). D) The deletion mutant *A. actinomycetemcomitans* strain D7S Δ*pilA::spe*^{r} induced less ROS production from isolated human neutrophils than the parental wild strain D7S (p = 0.005; Mann–Whitney *U* test with Bonferroni correction) and the wild-type strain D11S (p = 0.008; Mann–Whitney *U* test with Bonferroni correction).

specific antibodies than healthy control subjects [45]. However, there are nonsignificant amounts of specific antibodies against outer membrane secretin emHofQ [40] or outer membrane lipoprotein bacterial interleukin receptor I (BilRI) [45]. Therefore, we measured whether PilA, which likely spans the outer membrane, could elicit antibody production. The levels of AaPilA-specific antibodies were higher in the sera of *A. actinomycetemcomitans*-positive patients than in the sera of healthy controls (p = 0.034, Mann–Whitney *U* test) (Fig. 4C).

3.7. PilA induces leukocyte ROS production

Because PilA likely passes the outer membrane of *A. actinomycetemcomitans*, it encounters host cells in host-microbe interactions. Therefore, we studied the interactions of AaPilA with human leukocytes from healthy volunteers. Freshly isolated human leukocytes were incubated with whole *A. actinomycetemcomitans* cells: two wild-type strains expressing the two most common PilA variants (D7S and D11S), and deletion mutant D7S Δ*pilA::spe*^{r}. The ROS production induced by deletion mutant D7S Δ*pilA::spe*^{r} was significantly lower than the ROS production induced by wild-type strains D7S and D11S (p = 0.005 and p = 0.008, respectively; Mann–Whitney *U* test with Bonferroni correction). There was no significant difference between the two wild-type strains (p = 1.00; Mann–Whitney *U* test with Bonferroni correction) (Fig. 4D).

3.8. Recombinant PilA does not induce cytokine secretion in human macrophages

The immunogenic properties of AaPilA were further tested with human macrophages. N-terminally truncated recombinant PilAD7S (Δ1–27) did not induce cytokine secretion and was not cytotoxic. Bacterial lipopolysaccharide (LPS) from *A. actinomycetemcomitans* induced the secretion of IL-6 and TNF-α (p = 0.02; Mann–Whitney *U* test with Bonferroni correction) and reduced cell viability. Since there were differences between the cytotoxicity of AaPilA and AaLPS, the amounts of cytokines were related to cell viability (Table 2).

We also measured the amount of IL-8 in some of the samples. The secretion of IL-8 did not increase significantly in the presence of bacterial agents (data not shown). However, in the nonstimulated control samples, the basal level of IL-8 (130–160 ng) was higher than the basal level of IL-6 (3–7 ng) or TNF-α (17–38 ng).

4. Discussion

Binding of extracellular DNA followed by DNA uptake and natural transformation is mediated by type IV pili in gram-negative species [3,4,20]. DNA-binding by type IV pilins has been shown to be mediated by electropositivity rather than a specific structural domain, and the DNA-binding site resides on the C-terminal globular domain of the pilin [18,65]. Our results show that recombinant PilAD7S(Δ1–27), an N-terminally truncated variant of the major pilin protein that is present in naturally competent *A. actinomycetemcomitans* strains (D7S, 624, D17P-3 [1]), is capable of binding linear DNA. AaPilA has positively charged lysines (K) in the C-terminal domain, which can bind negatively charged DNA. Our findings support the important role of PilA in the natural transformation of *A. actinomycetemcomitans*, which was previously shown by Wang and coworkers [35]. As noncompetent strains are incapable of incorporating DNA into their genome after losing some function(s) in genes related to regulation, DNA uptake or transformation [1], it was not of interest to study DNA binding with other variants.

Table 2
Recombinant N-terminally truncated PilA (0.1 ng/ml) did not stimulate IL-6 or TNF-α production from the human macrophage cell line THP-1. *A. actinomycetemcomitans* LPS (0.1 ng/ml) was used as a positive control. The growth medium was collected for cytokine quantification with ELISA after either 6 h or 24 h of stimulation. Cell viability was measured with the neutral red uptake assay, and the measured cytokine amounts were related to the respective cell viabilities. P values were calculated with a pairwise Mann–Whitney *U* test with Bonferroni correction (n = 2).

		relative cell viability		IL-6 (pg)	*IL-6 (pg)/ viability*	
6 h	**control**	1.00 ± 0.00		3.16 ± 1.95	3.16 ± 1.95	
	PilAD7S (Δ1–27)	1.09 ± 0.08		2.13 ± 1.75	1.98 ± 1.61	
	Aa LPS	0.66 ± 0.33		36.92 ± 24.26	65.39 ± 39.43	p = 0.02
24 h	**control**	1.00 ± 0.00		3.82 ± 4.89	3.82 ± 4.89	
	PilAD7S (Δ1–27)	1.07 ± 0.10		2.03 ± 1.60	2.02 ± 1.71	
	Aa LPS	0.59 ± 0.27	p = 0.01	147.57 ± 96.07	278.48 ± 153.32	p = 0.02
		relative cell viability		**TNF-α (pg)**	**TNF-α (pg)/ viability**	
6 h	**control**	1.00 ± 0.00		34.49 ± 60.54	34.49 ± 60.54	
	PilAD7S (Δ1–27)	1.09 ± 0.08		48.19 ± 68.19	48.83 ± 72.76	
	Aa LPS	0.66 ± 0.33		1130.44 ± 727.70	1840.16 ± 729.46	p = 0.02
24 h	**control**	1.00 ± 0.00		9.4 ± 16.86	9.40 ± 16.86	
	PilAD7S (Δ1–27)	1.07 ± 0.10		6.76 ± 10.89	7.14 ± 11.85	
	Aa LPS	0.59 ± 0.27	p = 0.01	1083.71 ± 963.96	1924.31 ± 1256.12	p = 0.02

Values are presented as the average ± standard deviation (n = 5).

In this study, we showed that *A. actinomycetemcomitans* PilA possesses immunogenic properties, making it a potential virulence factor. The deletion mutant devoid of the *pilA* gene could not stimulate ROS production from isolated human leukocytes as effectively as the wild-type *A. actinomycetemcomitans* cells. The two wild-type strains, D7S and D11S, express the two most common PilA variants, but their ability to induce ROS production was similar. It has been shown that *A. actinomycetemcomitans* serotype b LPS primes human neutrophils for ROS production, similar to *E. coli* LPS [66]. The *A. actinomycetemcomitans* strains D7S and D11S belong to serotype groups a and c, respectively [41,42], suggesting that serotype a LPS present in the Δ*pilA::spe*^{r} strain might be a poorer ROS inducer than serotype b LPS. However, the most likely explanation is that the cell-bound serotype LPS cannot induce ROS production, similar to the purified LPS used in the study by Aida and coworkers [66], since the lipid-A moiety is necessary for priming [66]. Although the PilA protein is involved in the stimulation of ROS production, other outer membrane proteins BilRI and emHofQ, which most likely belong to the same DNA uptake machinery [1,39,45], do not have similar roles [40,45].

While PilA induced ROS production in human leukocytes, the recombinant, N-terminally truncated PilAD7S(Δ1–27) was not able to induce cytokine secretion from human THP-1 macrophages. However, the results show only that a single C-terminal globular domain of PilA cannot stimulate macrophages. In natural settings, similar pilin proteins form pilus filaments consisting of multiple subunits. Although full-length recombinant AaPilA formed large complexes, they are likely nonnative protein aggregates because a specific biogenesis machinery is needed to form pilus filaments [3,67]. Additionally, producing a full-length PilA without a His-tag proved to be difficult, as the highly hydrophobic N-terminus decreased the solubility and most likely formed complexes with *E. coli* proteins. However, N-terminally truncated recombinant pilin proteins have previously been successfully used in functional as well as structural studies, as the N-terminal truncation prevents aggregation but leaves the C-terminal functional domain intact [18,68,69].

Recombinant PilAD7S(Δ1–27) was nontoxic to human macrophages, unlike proinflammatory cytokine production-inducing molecules, such as LPS and leukotoxin. Proinflammatory cytokines that are involved in periodontitis include the IL-1β, IL-6 and TNF families [70]. *A. actinomycetemcomitans* possesses various proinflammatory virulence factors, such as LPS, cytolethal distending toxin (CDT), leukotoxin, and peptidoglycan-associated lipoprotein [71–73], which have the potential to stimulate the production of these cytokines. All three subunits of CDT, CdtA, CdtB and CdtC were able to stimulate the production of IL-1β, IL-6 and IL-8 by human peripheral blood mononuclear cells [74]. The *A. actinomycetemcomitans* outer membrane most likely contains larger amounts of the other proinflammatory molecules, such as LPS, than PilA, which is expressed only under conditions that stimulate natural transformation [35].

Although *A. actinomycetemcomitans* PilA did not induce the production of IL-6, TNF-α, or IL-8 in our experimental setup, PilA could bind IL-8 and TNF-α. N-terminally truncated PilAD7S(Δ1–27) was used to study the interaction between PilA and cytokines to avoid unreliable results due to protein aggregation. The cytokine binding assays used in this study are based on His-tag recognition, and therefore multiple His-tags may give signals that are too high. Binding was tested only with the PilAD7S variant, which is present in naturally competent strains, as we have previously proposed a link between DNA and cytokine uptake [40]. The dissociation constants for IL-8 and TNF-α were 0.67 ± 0.18 μM and 7.16 ± 0.40 μM, respectively. This indicates that their binding to PilA was relatively loose, which is typical for transient interactions. We have previously shown that two other outer membrane proteins of *A. actinomycetemcomitans*, the lipoprotein BilRI and secretin channel HofQ, which are involved in the uptake of eDNA, are able to bind various cytokines [38,40]. The dissociation constant between HofQ and IL-8 was 43 ± 4 nM, but the interaction between BilRI and IL-8 could not be determined due to weak interactions [75]. However, in the same study, we showed that outer membrane LPS could bind IL-8 with a dissociation constant varying from 1.2 to 17 μM [75]. Moreover, IL-8 interacts with dsDNA, most likely due to the opposite net charges of these two molecules [40]. The affinities to IL-8 increase logically in the proposed order of binding from LPS to PilA and finally to HofQ.

The results of this study strengthen our earlier hypothesis that the DNA uptake machinery of *A. actinomycetemcomitans* is involved in the sequestration of inflammatory cytokines [40]. A similar link between cytokine uptake and the type IVa pilus has also been shown in *N. meningitidis* [19]. The expression of the proteins that form the competence machinery is most likely regulated by catabolite repression in *A. actinomycetemcomitans* [64]. Therefore, these proteins are not constitutively expressed, and cytokine sequestration is turned on or off depending on the conditions. To fully understand the various functions of the type IVa pilus-producing machinery, more information is needed about the regulation of these genes. Undoubtedly, *A. actinomycetemcomitans* PilA is a potent virulence factor since, when stimulated with PilA, human immune cells produce a wide arsenal of weapons, including ROS and antibodies. Small molecules that are targeted against the gene regulation of *pilA* or the specific binding sites in PilA, which interact with human receptors and cytokines, might be potential antivirulence drug candidates. However, detailed studies are needed to elucidate these interaction sites.

Funding

This work was supported by the Academy of Finland under grants 265609, 272960, 303781, 322817; Federation of European

Microbiological Societies; The Magnus Ehrnrooth foundation; Turku University Foundation; The Paulo Foundation; County Council of Västerbotten, Sweden under grant 7003193.

CRediT authorship contribution statement

Nelli Vahvelainen: Writing – original draft, Visualization, Investigation, Formal analysis, Data curation. **Esra Bozkurt:** Writing – original draft, Visualization, Resources, Methodology, Investigation, Formal analysis, Data curation, Conceptualization. **Terhi Maula:** Writing – review & editing, Supervision, Methodology, Investigation, Funding acquisition, Formal analysis. **Anders Johansson:** Writing – review & editing, Supervision, Resources, Methodology, Funding acquisition, Conceptualization. **Marja T. Pöllänen:** Writing – review & editing, Supervision, Resources, Project administration, Methodology, Conceptualization. **Riikka Ihalin:** Writing – review & editing, Writing – original draft, Supervision, Resources, Project administration, Methodology, Investigation, Funding acquisition, Conceptualization.

Declaration of competing interest

The authors declare that they have no known competing financial interests or personal relationships that could have appeared to influence the work reported in this paper.

Data availability

The dataset related to the computational modeling of *A. actinomycetemcomitans* PilA is openly available in the Dryad repository (https://datadryad.org) with DOI https://doi.org/10.5061/dryad.w6m905qqz.

Acknowledgments

The authors would like to thank computer resources in the projects (snic2021-22-620 and snic2021-5-376) provided by the Swedish National Infrastructure for Computing (SNIC) at UPPMAX. MSc Laura Kovesjoki is thanked for her skillful technical assistance in ELISA measurements of specific antibody levels in human sera and Adjunct Professor Jari Nuutila for supervising the ROS measurement assays.

Appendix A. Supplementary data

Supplementary data to this article can be found online at https://doi.org/10.1016/j.micpath.2022.105843.

References

[1] P. Jorth, M. Whiteley, An evolutionary link between natural transformation and crispr adaptive immunity, mBio 3 (2012), https://doi.org/10.1128/mBio.00309-12.
[2] K.H. Piepenbrink, DNA uptake by type IV filaments, Front. Mol. Biosci. 6 (2019) 1, https://doi.org/10.3389/fmolb.2019.00001.
[3] L. Craig, K.T. Forest, B. Maier, Type IV pili: dynamics, biophysics and functional consequences, Nat. Rev. Microbiol. 17 (2019) 429–440, https://doi.org/10.1038/s41579-019-0195-4.
[4] I. Chen, D. Dubnau, DNA uptake during bacterial transformation, Nat. Rev. Microbiol. 2 (2004) 241–249, https://doi.org/10.1038/nrmicro844.
[5] I. Chen, R. Provvedi, D. Dubnau, A macromolecular complex formed by a pilin-like protein in competent Bacillus subtilis, J. Biol. Chem. 281 (2006) 21720–21727, https://doi.org/10.1074/JBC.M604071200.
[6] K.P. Obergfell, H.S. Seifert, The pilin N-terminal domain maintains Neisseria gonorrhoeae transformation competence during pilus phase variation, PLoS Genet. 12 (2016), e1006069, https://doi.org/10.1371/JOURNAL.PGEN.1006069.
[7] C.D. Long, D.M. Tobiason, M.P. Lazio, K.A. Kline, H.S. Seifert, Low-level pilin expression allows for substantial DNA transformation competence in Neisseria gonorrhoeae, Infect. Immun. 71 (2003) 6279, https://doi.org/10.1128/IAI.71.11.6279-6291.2003.
[8] C.K. Ellison, T.N. Dalia, A. Vidal Ceballos, J.C.Y. Wang, N. Biais, Y.v. Brun, A. B. Dalia, Retraction of DNA-bound type IV competence pili initiates DNA uptake during natural transformation in Vibrio cholerae, Nat Microbiol. 3 (2018) 773–780, https://doi.org/10.1038/s41564-018-0174-y.
[9] M.D. Carruthers, E.N. Tracy, A.C. Dickson, K.B. Ganser, R.S. Munson, L.O. Bakaletz, Biological roles of nontypeable Haemophilus influenzae type IV pilus proteins encoded by the pil and com operons, J. Bacteriol. 194 (2012) 1927–1933, https://doi.org/10.1128/JB.06540-11.
[10] J.L. Berry, V. Pelicic, Exceptionally widespread nanomachines composed of type IV pilins: the prokaryotic Swiss Army knives, FEMS Microbiol. Rev. 39 (2015) 134–154, https://doi.org/10.1093/femsre/fuu001.
[11] A.L. Forslund, E.N. Salomonsson, I. Golovliov, K. Kuoppa, S. Michell, R. Titball, P. Oyston, L. Noppa, A. Sjöstedt, Å. Forsberg, The type IV pilin, PilA, is required for full virulence of Francisella tularensis subspecies tularensis, BMC Microbiol. 10 (2010) 227, https://doi.org/10.1186/1471-2180-10-227.
[12] P.J. Fernandes, Q. Guo, D.M. Waag, M.S. Donnenberg, The type IV pilin of Burkholderia mallei is highly immunogenic but fails to protect against lethal aerosol challenge in a murine model, Infect. Immun. 75 (2007) 3027–3032, https://doi.org/10.1128/IAI.00150-07.
[13] A.E. Essex-Lopresti, J.A. Boddey, R. Thomas, M.P. Smith, M.G. Hartley, T. Atkins, N.F. Brown, C.H. Tsang, I.R.A. Peak, J. Hill, I.R. Beacham, R.W. Titball, A type IV pilin, pilA, contributes to adherence of Burkholderia pseudomallei and virulence in vivo, Infect. Immun. 73 (2005) 1260–1264, https://doi.org/10.1128/IAI.73.2.1260-1264.2005.
[14] T.E. Kehl-Fie, S.E. Miller, J.W. st Geme, Kingella kingae expresses type IV pili that mediate adherence to respiratory epithelial and synovial cells, J. Bacteriol. 190 (2008) 7157–7163, https://doi.org/10.1128/JB.00884-08.
[15] K.H. Piepenbrink, E. Lillehoj, C.M. Harding, J.W. Labonte, X. Zuo, C.A. Rapp, R. S. Munson, S.E. Goldblum, M.F. Feldman, J.J. Gray, E.J. Sundberg, Structural diversity in the type IV Pili of multidrug-resistant acinetobacter, J. Biol. Chem. 291 (2016) 22924–22935, https://doi.org/10.1074/jbc.M116.751099.
[16] S.C. Bernard, N. Simpson, O. Join-Lambert, C. Federici, M.P. Laran-Chich, N. Maïssa, H. Bouzinba-Ségard, P.C. Morand, F. Chretien, S. Taouji, E. Chevet, S. Janel, F. Lafont, M. Coureuil, A. Segura, F. Niedergang, S. Marullo, P. O. Couraud, X. Nassif, S. Bourdoulous, Pathogenic Neisseria meningitidis utilizes CD147 for vascular colonization, Nat. Med. 20 (2014) 725–731, https://doi.org/10.1038/nm.3563.
[17] J.A. Jurcisek, J.E. Bookwalter, B.D. Baker, S. Fernandez, L.A. Novotny, R. S. Munson, L.O. Bakaletz, The PilA protein of non-typeable Haemophilus influenzae plays a role in biofilm formation, adherence to epithelial cells and colonization of the mammalian upper respiratory tract, Mol. Microbiol. 65 (2007) 1288–1299, https://doi.org/10.1111/j.1365-2958.2007.05864.x.
[18] A. Cehovin, P.J. Simpson, M.A. McDowell, D.R. Brown, R. Noschese, M. Pallett, J. Brady, G.S. Baldwin, S.M. Lea, S.J. Matthews, V. Pelicic, Specific DNA recognition mediated by a type IV pilin, Proc. Natl. Acad. Sci. U. S. A. 110 (2013) 3065–3070, https://doi.org/10.1073/pnas.1218832110.
[19] J. Mahdavi, P.J. Royer, H.S. Sjölinder, S. Azimi, T. Self, J. Stoof, L.M. Wheldon, K. Brännström, R. Wilson, J. Moreton, J.W.B. Moir, C. Sihlbom, T. Borén, A. B. Jonsson, P. Soultanas, D.A.A. Ala'Aldeen, Pro-inflammatory cytokines can act as intracellular modulators of commensal bacterial virulence, Open Biol. 3 (2013), 130048, https://doi.org/10.1098/rsob.130048.
[20] C.L. Giltner, Y. Nguyen, L.L. Burrows, Type IV pilin proteins: versatile molecular modules, Microbiol. Mol. Biol. Rev. 76 (2012) 740–772, https://doi.org/10.1128/mmbr.00035-12.
[21] C.K. Ellison, J. Kan, R.S. Dillard, D.T. Kysela, A. Ducret, C. Berne, C.M. Hampton, Z. Ke, E.R. Wright, N. Biais, A.B. Dalia, Y.v. Brun, Obstruction of pilus retraction stimulates bacterial surface sensing, Science 358 (2017) (1979) 535–538, https://doi.org/10.1126/science.aan5706.
[22] C.K. Ellison, J. Kan, J.L. Chlebek, K.R. Hummels, G. Panis, P.H. Viollier, N. Biais, A. B. Dalia, Y.v. Brun, A bifunctional ATPase drives tad pilus extension and retraction, Sci. Adv. 5 (2019), https://doi.org/10.1126/SCIADV.AAY2591.
[23] V. Pelicic, Type IV pili: e pluribus unum? Mol. Microbiol. 68 (2008) 827–837, https://doi.org/10.1111/j.1365-2958.2008.06197.x.
[24] S.C. Kachlany, P.J. Planet, R. DeSalle, D.H. Fine, D.H. Figurski, J.B. Kaplan, Flp-1, the first representative of a new pilin gene subfamily, is required for non-specific adherence of Actinobacillus actinomycetemcomitans, Mol. Microbiol. 40 (2001) 542–554, https://doi.org/10.1046/j.1365-2958.2001.02422.x.
[25] H.E. Parge, K.T. Forest, M.J. Hickey, D.A. Christensen, E.D. Getzoff, J.A. Tainer, Structure of the fibre-forming protein pilin at 2.6 Å resolution, Nature 378 (1995) 32–38, https://doi.org/10.1038/378032a0.
[26] L. Craig, R.K. Taylor, M.E. Pique, B.D. Adair, A.S. Arvai, M. Singh, S.J. Lloyd, D. S. Shin, E.D. Getzoff, M. Yeager, K.T. Forest, J.A. Tainer, Type IV pilin structure and assembly: X-ray and EM analyses of Vibrio cholerae toxin-coregulated pilus and Pseudomonas aeruginosa PAK pilin, Mol Cell. 11 (2003) 1139–1150, https://doi.org/10.1016/S1097-2765(03)00170-9.
[27] L. Craig, N. Volkmann, A.S. Arvai, M.E. Pique, M. Yeager, E.H.H. Egelman, J. A. Tainer, Type IV pilus structure by cryo-electron microscopy and crystallography: implications for pilus assembly and functions, Mol Cell. 23 (2006) 651–662, https://doi.org/10.1016/j.molcel.2006.07.004.
[28] S. Hartung, A.S. Arvai, T. Wood, S. Kolappan, D.S. Shin, L. Craig, J.A. Tainer, Ultrahigh resolution and full-length pilin structures with insights for filament assembly, pathogenic functions, and vaccine potential, J. Biol. Chem. 286 (2011) 44254–44265, https://doi.org/10.1074/jbc.M111.297242.
[29] S. Kolappan, M. Coureuil, X. Yu, X. Nassif, E.H. Egelman, L. Craig, Structure of the Neisseria meningitidis type IV pilus, Nat. Commun. 7 (2016), 13015, https://doi.org/10.1038/ncomms13015.
[30] F. Wang, M. Coureuil, T. Osinski, A. Orlova, T. Altindal, G. Gesbert, X. Nassif, E. H. Egelman, L. Craig, Cryoelectron microscopy reconstructions of the Pseudomonas

aeruginosa and Neisseria gonorrhoeae type IV pili at sub-nanometer resolution, Structure 25 (2017) 1423–1435, https://doi.org/10.1016/j.str.2017.07.016, e4.
[31] B. Bardiaux, G.C. de Amorim, A. Luna Rico, W. Zheng, I. Guilvout, C. Jollivet, M. Nilges, E.H. Egelman, N. Izadi-Pruneyre, O. Francetic, Structure and assembly of the enterohemorrhagic Escherichia coli type 4 pilus, Structure 27 (2019) 1082–1093, https://doi.org/10.1016/j.str.2019.03.021, e5.
[32] N. Roux, J. Spagnolo, S. de Bentzmann, Neglected but amazingly diverse type IVb pili, Res. Microbiol. 163 (2012) 659–673, https://doi.org/10.1016/j.resmic.2012.10.015.
[33] R.J. Lamont, H. Koo, G. Hajishengallis, The oral microbiota: dynamic communities and host interactions, Nat. Rev. Microbiol. 16 (2018) 745–759, https://doi.org/10.1038/s41579-018-0089-x.
[34] M.T. Villar, R.L. Hirschberg, M.R. Schaefer, Role of the Eikenella corrodens pilA locus in pilus function and phase variation, J. Bacteriol. 183 (2001) 55–62, https://doi.org/10.1128/JB.183.1.55-62.2001.
[35] Y. Wang, W. Shi, W. Chen, C. Chen, Type IV pilus gene homologs pilABCD are required for natural transformation in Actinobacillus actinomycetemcomitans, Gene 312 (2003) 249–255, https://doi.org/10.1016/S0378-1119(03)00620-6.
[36] A. Paino, H. Tuominen, M. Jääskeläinen, J. Alanko, J. Nuutila, S.E. Asikainen, L. J. Pelliniemi, M.T. Pöllänen, C. Chen, R. Ihalin, Trimeric form of intracellular ATP synthase subunit β of aggregatibacter actinomycetemcomitans binds human interleukin-1β, PLoS One 6 (2011) https://doi.org/10.1371/journal.pone.0018929.
[37] A. Paino, E. Lohermaa, R. Sormunen, H. Tuominen, J. Korhonen, M.T. Pöllänen, R. Ihalin, Interleukin-1β is internalised by viable Aggregatibacter actinomycetemcomitans biofilm and locates to the outer edges of nucleoids, Cytokine 60 (2012) 565–574, https://doi.org/10.1016/j.cyto.2012.07.024.
[38] T. Ahlstrand, H. Tuominen, A. Beklen, A. Torittu, J. Oscarsson, R. Sormunen, M. T. Pöllänen, P. Permi, R. Ihalin, A novel intrinsically disordered outer membrane lipoprotein of Aggregatibacter actinomycetemcomitans binds various cytokines and plays a role in biofilm response to interleukin-1β and interleukin-8, Virulence 8 (2017) 115–134, https://doi.org/10.1080/21505594.2016.1216294.
[39] M. Tarry, M. Jääskeläinen, A. Paino, H. Tuominen, R. Ihalin, M. Högbom, The extra-membranous domains of the competence protein HofQ show DNA binding, flexibility and a shared fold with type i KH domains, J. Mol. Biol. 409 (2011) 642–653, https://doi.org/10.1016/j.jmb.2011.04.034.
[40] T. Ahlstrand, A. Torittu, H. Elovaara, H. Välimaa, M.T. Pöllänen, S. Kasvandik, M. Högbom, R. Ihalin, Interactions between the Aggregatibacter actinomycetemcomitans secretin HofQ and host cytokines indicate a link between natural competence and interleukin-8 uptake, Virulence 9 (2018) 1205–1223, https://doi.org/10.1080/21505594.2018.1499378.
[41] C. Chen, W. Kittichotirat, W. Chen, J.S. Downey, Y. Si, R. Bumgarner, Genome sequence of naturally competent Aggregatibacter actinomycetemcomitans serotype a strain D7S-1, J. Bacteriol. 192 (2010) 2643–2644, https://doi.org/10.1128/JB.00157-10.
[42] C. Chen, W. Kittichotirat, Y. Si, R. Bumgarner, Genome Sequence of Aggregatibacter Actinomycetemcomitans Serotype C Strain D11S-1, 191, 2009, pp. 7378–7379, https://doi.org/10.1128/JB.01203-09.
[43] O.H. Lowry, N.J. Rosebrough, A.L. Farr, R.J. Randall, Protein measurement with the Folin phenol reagent, J. Biol. Chem. 193 (1951) 265–275, https://doi.org/10.1016/s0021-9258(19)52451-6.
[44] E.M.E. Lilius, J.T.J. Nuutila, Particle-induced myeloperoxidase release in serially diluted whole blood quantifies the number and the phagocytic activity of blood neutrophils and opsonization capacity of plasma, Luminescence 21 (2006) 148–158, https://doi.org/10.1002/bio.899.
[45] T. Maula, N. Vahvelainen, H. Tossavainen, T. Koivunen, M.T. Pöllänen, A. Johansson, P. Permi, R. Ihalin, Decreased temperature increases the expression of a disordered bacterial late embryogenesis abundant (LEA) protein that enhances natural transformation, Virulence 12 (2021) 1239–1257, https://doi.org/10.1080/21505594.2021.1918497.
[46] S. Tsuchiya, M. Yamabe, Y. Yamaguchi, Y. Kobayashi, T. Konno, K. Tada, Establishment and characterization of a human acute monocytic leukemia cell line (THP-1), Int. J. Cancer 26 (1980) 171–176, https://doi.org/10.1002/ijc.2910260208.
[47] G.N. Belibasakis, A. Johansson, Y. Wang, C. Chen, S. Kalfas, U.H. Lerner, The cytolethal distending toxin induces receptor activator of NF-κB ligand expression in human gingival fibroblasts and periodontal ligament cells, Infect. Immun. 73 (2005) 342–351, https://doi.org/10.1128/IAI.73.1.342-351.2005.
[48] G. Repetto, A. del Peso, J.L. Zurita, Neutral red uptake assay for the estimation of cell viability/cytotoxicity, Nat. Protoc. 3 (2008) 1125–1131, https://doi.org/10.1038/nprot.2008.75.
[49] S.F. Altschul, W. Gish, W. Miller, E.W. Myers, D.J. Lipman, Basic local alignment search tool, J. Mol. Biol. 215 (1990) 403–410, https://doi.org/10.1016/S0022-2836(05)80360-2.
[50] F. Madeira, Y.M. Park, J. Lee, N. Buso, T. Gur, N. Madhusoodanan, P. Basutkar, A. R.N. Tivey, S.C. Potter, R.D. Finn, R. Lopez, The EMBL-EBI search and sequence analysis tools APIs in 2019, Nucleic Acids Res. 47 (2019) W636–W641, https://doi.org/10.1093/nar/gkz268.
[51] G. Waksman, Structural and molecular biology of a protein-polymerizing nanomachine for pilus biogenesis, J. Mol. Biol. 429 (2017) 2654–2666, https://doi.org/10.1016/J.JMB.2017.05.016.
[52] J. Jumper, R. Evans, A. Pritzel, T. Green, M. Figurnov, O. Ronneberger, K. Tunyasuvunakool, R. Bates, A. Žídek, A. Potapenko, A. Bridgland, C. Meyer, S.A. A. Kohl, A.J. Ballard, A. Cowie, B. Romera-Paredes, S. Nikolov, R. Jain, J. Adler, T. Back, S. Petersen, D. Reiman, E. Clancy, M. Zielinski, M. Steinegger, M. Pacholska, T. Berghammer, S. Bodenstein, D. Silver, O. Vinyals, A.W. Senior, K. Kavukcuoglu, P. Kohli, D. Hassabis, Highly accurate protein structure prediction with AlphaFold, Nature 596 (2021) 583–589, https://doi.org/10.1038/s41586-021-03819-2.
[53] J.C. Gordon, J.B. Myers, T. Folta, V. Shoja, L.S. Heath, A. Onufriev, H++: a server for estimating pKas and adding missing hydrogens to macromolecules, Nucleic Acids Res. 33 (2005), https://doi.org/10.1093/nar/gki464.
[54] T.S. Lee, D.S. Cerutti, D. Mermelstein, C. Lin, S. Legrand, T.J. Giese, A. Roitberg, D. A. Case, R.C. Walker, D.M. York, GPU-accelerated molecular dynamics and free energy methods in Amber18: performance enhancements and new features, J. Chem. Inf. Model. 58 (2018) 2043–2050, https://doi.org/10.1021/acs.jcim.8b00462.
[55] J.A. Maier, C. Martinez, K. Kasavajhala, L. Wickstrom, K.E. Hauser, C. Simmerling, ff14SB: improving the accuracy of protein side chain and backbone parameters from ff99SB, J. Chem. Theor. Comput. 11 (2015) 3696–3713, https://doi.org/10.1021/acs.jctc.5b00255.
[56] P. Mark, L. Nilsson, Structure and dynamics of the TIP3P, SPC, and SPC/E water models at 298 K, J. Phys. Chem. A 105 (2001) 9954–9960, https://doi.org/10.1021/jp003020w.
[57] J.A. Izaguirre, D.P. Catarello, J.M. Wozniak, R.D. Skeel, Langevin stabilization of molecular dynamics, J. Chem. Phys. 114 (2001) 2090–2098, https://doi.org/10.1063/1.1332996.
[58] T. Darden, D. York, L. Pedersen, Particle mesh Ewald: an N·log(N) method for Ewald sums in large systems, J. Chem. Phys. 98 (1993) 10089–10092, https://doi.org/10.1063/1.464397.
[59] H.G. Petersen, Accuracy and efficiency of the particle mesh Ewald method, J. Chem. Phys. 103 (1995) 3668–3679, https://doi.org/10.1063/1.470043.
[60] S. Miyamoto, P.A. Kollman, Settle: an analytical version of the SHAKE and RATTLE algorithm for rigid water models, J. Comput. Chem. 13 (1992) 952–962, https://doi.org/10.1002/jcc.540130805.
[61] D.R. Roe, T.E. Cheatham, PTRAJ and CPPTRAJ: software for processing and analysis of molecular dynamics trajectory data, J. Chem. Theor. Comput. 9 (2013) 3084–3095, https://doi.org/10.1021/ct400341p.
[62] D.R. Roe, T.E. Cheatham, Parallelization of CPPTRAJ enables large scale analysis of molecular dynamics trajectory data, J. Comput. Chem. 39 (2018) 2110–2117, https://doi.org/10.1002/jcc.25382.
[63] O. Fujise, L. Lakio, Y. Wang, S. Asikainen, C. Chen, Clonal distribution of natural competence in Actinobacillus actinomycetemcomitans, Oral Microbiol. Immunol. 19 (2004) 340–342, https://doi.org/10.1111/J.1399-302X.2004.00157.X.
[64] Y. Wang, S.D. Goodman, R.J. Redfield, C. Chen, Natural transformation and DNA uptake signal sequences in Actinobacillus actinomycetemcomitans, J. Bacteriol. 184 (2002) 3442–3449, https://doi.org/10.1128/JB.184.13.3442-3449.2002.
[65] E.J. van Schaik, C.L. Giltner, G.F. Audette, D.W. Keizer, D.L. Bautista, C. M. Slupsky, B.D. Sykes, R.T. Irvin, DNA binding: a novel function of Pseudomonas aeruginosa type IV pili, J. Bacteriol. 187 (2005) 1455–1464, https://doi.org/10.1128/JB.187.4.1455-1464.2005.
[66] Y. Aida, T. Kukita, H. Takada, K. Maeda, M.J. Pabst, Lipopolysaccharides from periodontal pathogens prime neutrophils for enhanced respiratory burst: differential effect of a synthetic lipid a Precursor IVA(LA-14-PP), J. Periodontal. Res. 30 (1995) 116–123, https://doi.org/10.1111/j.1600-0765.1995.tb01260.x.
[67] L. Craig, J. Li, Type IV pili: paradoxes in form and function, Curr. Opin. Struct. Biol. 18 (2008) 267–277, https://doi.org/10.1016/j.sbi.2007.12.009.
[68] B. Hazes, P.A. Sastry, K. Hayakawa, R.J. Read, R.T. Irvin, Crystal structure of Pseudomonas aeruginosa PAK pilin suggests a main-chain-dominated mode of receptor binding, J. Mol. Biol. 299 (2000) 1005–1017, https://doi.org/10.1006/JMBI.2000.3801.
[69] S. Helaine, D.H. Dyer, X. Nassif, V. Pelicic, K.T. Forest, 3D structure/function analysis of PilX reveals how minor pilins can modulate the virulence properties of type IV pili, Proc. Natl. Acad. Sci. U. S. A. 104 (2007) 15888–15893, https://doi.org/10.1073/PNAS.0707581104.
[70] W. Pan, Q. Wang, Q. Chen, The cytokine network involved in the host immune response to periodontitis, Int. J. Oral Sci. 11 (2019), https://doi.org/10.1038/S41368-019-0064-Z.
[71] G.N. Belibasakis, T. Maula, K. Bao, M. Lindholm, N. Bostanci, J. Oscarsson, R. Ihalin, A. Johansson, Virulence and pathogenicity properties of aggregatibacter actinomycetemcomitans, Pathogens 8 (2019) 222, https://doi.org/10.3390/PATHOGENS8040222.
[72] M. Paul-Satyaseela, M. Karched, Z. Bian, R. Ihalin, T. Borén, A. Arnqvist, C. Chen, S. Asikainen, Immunoproteomics of Actinobacillus actinomycetemcomitans outer-membrane proteins reveal a highly immunoreactive peptidoglycan-associated lipoprotein, J. Med. Microbiol. 55 (2006) 931–942, https://doi.org/10.1099/jmm.0.46470-0.
[73] R. Ihalin, K. Eneslätt, S. Asikainen, Peptidoglycan-associated lipoprotein of Aggregatibacter actinomycetemcomitans induces apoptosis and production of proinflammatory cytokines via TLR2 in murine macrophages RAW 264.7 in vitro, J. Oral Microbiol. 10 (2018), https://doi.org/10.1080/20002297.2018.1442079.
[74] S. Akifusa, S. Poole, J. Lewthwaite, B. Henderson, S.P. Nair, Recombinant Actinobacillus actinomycetemcomitans cytolethal distending toxin proteins are required to interact to inhibit human cell cycle progression and to stimulate human leukocyte cytokine synthesis, Infect. Immun. 69 (2001) 5925–5930, https://doi.org/10.1128/IAI.69.9.5925-5930.2001.
[75] T. Ahlstrand, L. Kovesjoki, T. Maula, J. Oscarsson, R. Ihalin, Aggregatibacter actinomycetemcomitans LPS binds human interleukin-8, J. Oral Microbiol. 11 (2019), 1549931, https://doi.org/10.1080/20002297.2018.1549931.